Int. J. Heat Mass Transfer. Vol. 30, No. 3, pp. 537–549, 1987
Printed in Great Britain

0017–9310/87 $3.00 + 0.00
Pergamon Journals Ltd.

Natural convection in a thin, inclined, porous layer exposed to a constant heat flux

P. VASSEUR, M. G. SATISH and L. ROBILLARD
Ecole Polytechnique, Montreal, P.Q., Canada H3C 3A7

(*Received* 30 *January* 1986 *and in final form* 9 *July* 1986)

Abstract—Thermally driven flow in a thin, inclined, rectangular cavity—filled with a fluid-saturated, porous layer—is studied analytically and numerically. A constant heat flux is applied for heating and cooling the two opposing walls of the layer while the other two walls are insulated. On the basis of the Darcy–Oberbeck–Boussinesq equations, the problem is solved analytically, in the limit of a thin layer, using asymptotic expansions and an integral form of the energy equation. Solutions for the flow fields, temperature distributions and Nusselt numbers are obtained explicitly in terms of the Rayleigh number and the angle of inclination of the cavity. A numerical study of the same phenomenon, obtained by solving the complete system of governing equations, is also conducted. A good agreement is found between the analytical predictions and the numerical simulation.

1. INTRODUCTION

OVER the past years considerable research efforts have been devoted to the study of heat transfer in cavities filled with a fluid-saturated, porous medium. To a large extent, this interest is stimulated by the fact that thermally driven flows in porous media are of considerable engineering interest. These problems arise in the design of pebble bed nuclear reactors, catalytic reactors, compact heat exchangers, solar power collectors, geothermal energy conversion, use of fibrous materials in the thermal insulation of buildings and geophysical flows. Another important area of application is heat transfer from the storage of agricultural products which generate heat as a result of metabolism. An excellent review of existing experimental and numerical results have been presented by Combarnous and Bories [1] and Catton [2].

The purpose of the present study is to examine the effects of natural convection in an inclined, rectangular, porous layer when a constant heat flux is applied on two opposing walls, while the other two walls are maintained adiabatic. The layer is referred to as being horizontal, vertical or tilted, depending on the orientation of its thermally active walls with respect to the gravity acceleration vector. A review of the literature shows that most previous theoretical publications deal with vertical [3–5] or horizontal [6, 7] cases. For situations involving inclined layers, available studies are relatively limited. The problem of a sloped porous layer, heated isothermally from below, has been considered theoretically and experimentally by Bories and Combarnous [8]. Depending on the values of the slope of the layer and the Rayleigh number, different shapes of free convection movements have been observed. Hence, a two-dimensional stable unicellular flow takes place in the layer if $R < 4\pi^2/\cos\phi$, where ϕ is the angle between the heated wall and the horizontal plane. On the other hand when the Rayleigh number is higher than this critical value a transition from unicellular flow to stable three-dimensional flow is observed. The resulting convective movements take then the form of polyhedral cells for ϕ lower than about 15° while for higher values of ϕ it consists of adjacent longitudinal coils climbing up along the direction of the slope. Finally for very high Rayleigh numbers it was found that, depending on the slope of the layer, a fluctuating regime or a wavy coils regime could be observed. Convection in a tilted, porous box—with two parallel isothermal planes and the other limits insulated—has been studied numerically by Vlasuk [9] for the range $A = 1$, $-90° < \phi < 90°$ and $R \leqslant 350$. It was found that the tilt angle, for maximum heat transfer, is approximately 50°. Holst and Aziz [10], considering temperature-dependent physical properties, investigated the heat transfer of a tilted square of porous material. Steady natural convection in a slightly inclined, rectangular, porous box has been studied by Walch and Dulieu [11] using the Galerkin method. A correlation for the Nusselt number as a function of Rayleigh number, aspect ratio and tilt angle has been obtained by these authors. More recently, the existence of multiple solutions, in a slightly inclined, porous cavity heated from the bottom, has been studied numerically by Walch and Dulieu [11], Moya *et al.* [12] and analytically by Caltagirone and Bories [13] who determined their stability. It was demonstrated that, for small angles of inclination, three different real solutions may exist for a given Rayleigh number and aspect ratio.

All the above studies have considered cavities with isothermal walls despite the fact that in many engineering applications the temperature of a wall is not uniform but, rather, is a result of the imposition

NOMENCLATURE

A	aspect ratio of the cavity, H'/L'
B	coefficient in equation (4.8) and equation (5.3)
C	temperature gradient along x direction
g	gravitational acceleration
H'	thickness of the cavity
k	thermal conductivity of fluid-saturated, porous medium
K	permeability
L'	length of the cavity
Nu	Nusselt number, equation (4.13)
p'	pressure
p	dimensionless pressure, $[p'/(\alpha\mu/k)]$
q'	constant heat flux
R	Rayleigh number, $g\beta KL^2q'/k\alpha\nu$
T'	temperature
T_0'	reference temperature at $x = y = 0$
ΔT	wall-to-wall temperature difference at $x = 0$, equation (4.12)
$\Delta T'$	characteristic temperature difference, $q'L'/k$
u'	velocity in x' direction
v'	velocity in y' direction
u	dimensionless velocity in x direction $(u'L'/\alpha)$
v	dimensionless velocity in y direction $(v'L'/\alpha)$
x'	coordinate axis along side walls (Fig. 1)
y'	coordinate axis along end walls (Fig. 1).
x	dimensionless coordinate axis (x'/L')
y	dimensionless coordinate axis (y'/L').

Greek symbols

α	effective thermal diffusivity
β	coefficient of thermal expansion
θ	temperature, equation (4.2)
ν	kinematic viscosity, μ/ρ
μ	dynamic viscosity
ρ	density
ψ	streamfunction
ϕ	angle of inclination of the enclosure.

Superscript

$'$	dimensional quantities.

Subscript

max	refers to maximum value.

of a constant heat flux. Results available for the situation where a constant heat flux is applied on one [14] or two [15] walls have been reported only for the case of a vertical cavity. The objective of the present work is to analyze the behavior of natural convection flows in rectangular, tilted, porous layers heated and cooled by constant heat fluxes. In the following sections, the differential equations, which describe the physical model considered here are formulated in a standard manner assuming the validity of Darcy's law and the Boussinesq approximation. An approximate solution, valid for long, shallow cavities is developed. The results of the analysis are verified through numerical calculations. The agreement between numerical results and the proposed analysis is found to be very good.

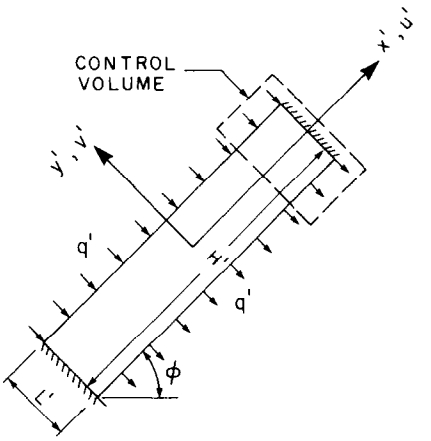

FIG. 1. Definition sketch.

2. STATEMENT OF THE PROBLEM

Consider the natural convective motion of a fluid filling a homogeneous, isotropic, porous medium confined on all sides by an impermeable rectangular box. The enclosure, shown in Fig. 1, is of height H', width L' and is tilted at an angle ϕ with respect to the horizontal plane. A uniform heat flux q' is applied along both side walls such that

$$q' = -k\frac{\partial T'}{\partial y'} \tag{2.1}$$

Here, k is the thermal conductivity of the porous medium, T' the temperature and primes denote dimensional variables. The two end walls are maintained adiabatic.

Assuming the validity of Darcy's law and the Boussinesq approximation and neglecting inertial effects, the equations describing conservation of mass, momentum and energy in the medium are, respectively

$$\frac{\partial u'}{\partial x'} + \frac{\partial v'}{\partial y'} = 0 \tag{2.2}$$

$$u' = -\frac{K}{\mu}\left(\frac{\partial p'}{\partial x'} + \rho g\cos\phi\right),$$

$$v' = -\frac{K}{\mu}\left(\frac{\partial p'}{\partial y'} - \rho g \sin\phi\right) \tag{2.3}$$

$$\frac{\partial^2 T'}{\partial x'^2} + \frac{\partial^2 T'}{\partial y'^2} = \frac{1}{\alpha}\left(u'\frac{\partial T'}{\partial x'} + v'\frac{\partial T'}{\partial y'}\right) \tag{2.4}$$

where u', v', p', g, K, μ and α stand for the velocity components in x' and y' directions, pressure, gravitational acceleration, medium permeability, viscosity and thermal diffusivity, respectively.

As usual, the governing equations are simplified if u' and v' are replaced by appropriately defining a streamfunction ψ' which satisfies the continuity equation (2.2) identically

$$u' = \frac{\partial \psi'}{\partial y'}, \qquad v' = -\frac{\partial \psi'}{\partial x'}. \tag{2.5}$$

Further, the pressure terms appearing in equation (2.3) are eliminated through cross-differentiation. The momentum and energy equations become:

$$\nabla^2 \psi' = \frac{-Kg\beta}{\nu}\left[\frac{\partial T'}{\partial x'}\cos\phi - \frac{\partial T'}{\partial y'}\sin\phi\right] \tag{2.6}$$

$$\nabla^2 T' = \frac{1}{\alpha}\left[\frac{\partial \psi'}{\partial y'}\frac{\partial T'}{\partial x'} - \frac{\partial \psi'}{\partial x'}\frac{\partial T'}{\partial y'}\right] \tag{2.7}$$

where ν is the kinematic viscosity μ/ρ.

Finally, equations (2.6) and (2.7) are put in a non-dimensional form by defining a new set of variables

$$(x, y) = (x', y')/L', \qquad \psi = \psi'/\alpha,$$
$$T = (T' - T_0')/\Delta T' \tag{2.8}$$

where T_0' is the temperature at the geometric center of the cavity and $\Delta T' = (q'L')/k$, a characteristic temperature difference.

The resulting equations for the streamfunction ψ and temperature T are:

$$\nabla^2 \psi = -R\left(\frac{\partial T}{\partial x}\cos\phi - \frac{\partial T}{\partial y}\sin\phi\right) \tag{2.9}$$

$$\nabla^2 T = \frac{\partial \psi}{\partial y}\frac{\partial T}{\partial x} - \frac{\partial \psi}{\partial x}\frac{\partial T}{\partial y} \tag{2.10}$$

where R is a Rayleigh number based on the constant heat flux q' and the permeability K of the medium

$$R = \frac{g\beta K L'^2 q'}{\alpha \nu k}. \tag{2.11}$$

The boundary conditions on ψ and T are:

$$\psi = 0 \qquad \frac{\partial T}{\partial x} = 0 \qquad \text{on } x = \pm A/2 \tag{2.12}$$

$$\psi = 0 \qquad \frac{\partial T}{\partial y} = 1 \qquad \text{on } y = \pm 1/2 \tag{2.13}$$

where $A = H'/L'$ is the cavity aspect ratio.

The problem is to find the functions ψ and T which satisfy the governing equations (2.9) and (2.10) and boundary conditions (2.12) and (2.13) for the case of a long shallow cavity, i.e. for the condition $A \gg 1$ with fixed values of R.

3. NUMERICAL SOLUTION

To obtain numerical solutions of the complete governing equations (2.9) and (2.10), finite differences were used. The solution consists of the streamfunction and temperature fields as well as the velocity distribution in x and y directions.

The energy equation was solved using the alternating direction implicit (ADI) method of Peaceman and Rachford [16]. The streamfunction field was obtained from equation (2.9) using the successive over-relaxation method (SOR) and a known temperature distribution. Forward time and central space differences were used and the advective term in the energy equation was written in conservative form to preserve the transportive property.

The number of grid points in the x and y directions were varied, depending upon the aspect ratio A of the cavity. As expected it was found that the necessary number of grid lines depended on the Rayleigh number R and the aspect ratio A of the cavity. Trial calculations were necessary in order to optimize computation time and accuracy. A grid of 51 × 51 was found to model accurately the flow fields described in the results for most of the cases considered. For instance, when $R = 250$, $\phi = 90°$ and $A = 4$, Nusselt numbers of 4.587 and 4.546 and maximum streamfunctions of 2.971 and 2.987 were obtained with 51 × 51 and 81 × 81 meshes, respectively. For very high aspect ratios a mesh of 81 × 81 was utilized in the present study.

The iterative procedure for the streamfunction was repeated until the following condition was satisfied:

$$\frac{\sum_i \sum_j |\psi_{i,j}^{n+1} - \psi_{i,j}^{n}|}{\sum_i \sum_j |\psi_{i,j}^{n+1}|} \leqslant 0.5 \times 10^{-3} \tag{3.1}$$

where the superscripts n and $(n + 1)$ indicate the value of the nth and $(n + 1)$th iterations respectively and i and j indices denote grid locations in the (x, y) plane. Further decrease of the convergence criteria (0.5×10^{-3}) did not cause any significant change in the final results.

The steady state was defined based on the following criteria:

$$\left|\frac{\psi_{\max}^{n+1} - \psi_{\max}^{n}}{\psi_{\max}^{n+1}}\right| \leqslant 0.5 \times 10^{-3} \tag{3.2}$$

where $\psi_{\max}$ is the maximum value of the streamfunction inside the cavity.

The number of iterations required for convergence was, in general, less than 1200. Convergence with mesh size was verified by employing coarser and finer

grids on selected test problems. Typical values of the time steps ranged from 10^{-3} to 10^{-4}. The CPU time required for convergence was from 180 to 1200 s on an IBM 4381 computer.

In order to verify the convergence of the present numerical study, some of the cases considered by Shiralkar *et al.* [5], for the natural convection in a vertical, rectangular, porous enclosure subjected to a horizontal temperature differential, were reproduced. In general it was found that essentially identical flow and temperature patterns as well as the average heat transfer were obtained. For instance, when $R = 500$ and $A = 2.25$, an overall Nusselt number of 9.998 was obtained in the present study while that reported by Shiralkar *et al.* was 10.073. As an additional check on the accuracy of the results, an energy balance was used for the system. For this the heat transfer through each plane $y =$ constant was evaluated at each location $-1/2 \leqslant y \leqslant 1/2$ and compared with the input at $y = 1/2$. For most of the results reported here the energy balance was satisfied to within 1–2%.

4. LAYER HEATED FROM THE SIDE WALLS

In this section an approximate solution to the governing equations (2.9) and (2.10) is sought for the case of a long, shallow cavity heated from the side by a constant heat flux. For this situation it is assumed that:

$$A \gg 1 \text{ with } R \text{ constant.} \tag{4.1}$$

The case of a long, shallow, horizontal, porous layer with the two vertical walls held at fixed but different temperatures and the horizontal surfaces maintained adiabatic has been studied in the past by Walker and Homsy [17]. By using matched asymptotic expansions it was shown that the flow inside the cavity may be decomposed into three parts; a core region of extent $O(A)$ in the center of the cavity, and two end regions within an $O(1)$ distance from the end walls. The solutions in the three regions are coupled by the matching requirements in the regions of overlap. Physically, the basic flow consists of a buoyancy-driven, parallel flow which is moderated by viscous effects over a length H'. The flow then turns through 180° in the end regions. This procedure will be followed in the present investigation in order to study both the effects of the inclination angle and the presence of constant heat fluxes imposed on two opposite walls.

As already discussed in refs. [17–19] for the case of a thin porous layer ($A \gg 1$) the flow within the core region of the cavity may be expected to be parallel. As a result the streamfunction and temperature field must be respectively of the following form [17]:

$$T = Cx + \theta(y) \tag{4.2}$$

and

$$\psi = \psi(y) \tag{4.3}$$

where C, the temperature gradient along the x direction, has to be determined from the thermal boundary conditions imposed on the end regions of the cavity.

Substituting equations (4.2) and (4.3) into equations (2.9) and (2.10) one obtains respectively:

$$\theta_{yyy} - \alpha^2\theta_y + \alpha^2 C\cot\phi = 0 \tag{4.4}$$

and

$$C\psi_y - \theta_{yy} = 0 \tag{4.5}$$

where $\alpha^2 = RC\sin\phi$.

Integrating equations (4.4) and (4.5) and making use of equation (4.2) and the boundary conditions from equation (2.13), one obtains respectively:

$$T = Cx + \frac{B}{\alpha}\sinh\alpha y + Cy\cot\phi \tag{4.6}$$

and

$$\psi = \frac{B}{C}(\cosh\alpha y - \cosh\alpha/2) \tag{4.7}$$

where

$$B = (1 - C\cot\phi)/\cosh\alpha/2. \tag{4.8}$$

The velocity component u is derived from equation (4.7) to be:

$$u = \frac{B\alpha}{C}\sinh\alpha y. \tag{4.9}$$

The value of the unknown constant C, the axial temperature gradient, has to be determined from the thermal boundary conditions imposed on the end walls. The constant C may be obtained in general by matching the core solution with solutions valid in the end regions. In the case of a porous cavity with isothermal end walls, such a solution has been developed formally by Walker and Homsy [17] and a first-order description of the entire flow field, including the corner interaction regions was obtained. However it was shown by Bejan and Tien [18] that, in order to determine the constant C, which defines the core flow, a detailed analysis of the end regions is not absolutely necessary. In fact the constant C may be evaluated simply by matching the core region with an integral solution for the flow and temperature field in the end region. In the case of a cavity with isothermal vertical walls, this was done by selecting reasonable profiles for the velocity and temperature distributions inside the end regions. In the present problem, due to the fact that a constant heat flux is imposed on the vertical walls, a guess of the velocity and temperature profiles inside the end regions is not even required to solve the core region [15]. The value of the constant C may be obtained simply by considering the arbitrary control volume of Fig. 1. Integration of equation (2.10), together with boundary

conditions (2.12) and (2.13), yields the following equation:

$$\int_{-1/2}^{1/2}\left[uT-\frac{\partial T}{\partial x}\right]dy=0 \tag{4.10}$$

at any position x.

Substituting equations (4.6), (4.8) and (4.9) into (4.10) and integrating yields:

$$C=\frac{B^2}{2C}\left(\frac{\sinh\alpha}{\alpha}-1\right)-B\cot\phi\cosh\alpha/2\left[\frac{2\tanh\alpha/2}{\alpha}-1\right]. \tag{4.11}$$

The value of the axial temperature gradient C may be evaluated, for a given Rayleigh number R and inclination angle ϕ from the above equation.

The Nusselt number predicted by the present analysis is derived by first evaluating the wall-to-wall dimensionless temperature difference, taken arbitrarily at the position $x = 0$ since the temperature of each thermally active wall varies linearly in x. Thus

$$\Delta T=T_{0,1/2}-T_{0,-1/2}=2T_{0,1/2}=\frac{2B}{\alpha}\sinh\frac{\alpha}{2}+C\cot\phi. \tag{4.12}$$

The Nusselt number Nu is given by

$$Nu=\left(\frac{q'}{\Delta\bar{T}}\right)\frac{L'}{k}=\frac{1}{\Delta\bar{T}}=\frac{\alpha}{2B\sinh\alpha/2+C\alpha\cot\phi} \tag{4.13}$$

where $\Delta\bar{T}$ is the actual wall-to-wall temperature difference.

Figure 2 presents the results for Nusselt number Nu as a function of the angle of inclination ϕ for Rayleigh numbers of 20, 100 and 500, respectively. No numerical results are presented for $R > 500$ since they did not provide sufficient additional insight into the problem and also the computing time necessary to obtain an accurate steady-state solution became rapidly prohibitive. Also shown in the figure are results of numerical calculations for cavities with aspect ratios $A = 3$, 4 and 5. An excellent agreement between the analytical and numerical results is observed in the range of the parameters considered. The orientation angle ϕ is seen to have a dominant effect on the Nusselt number for a given Rayleigh number. As the angle of inclination ϕ approaches 0°, the Nusselt number tends toward unity, indicating that the heat transfer is mainly due to conduction. This is expected since $\phi = 0°$ corresponds to the case of a cavity heated from the top which causes no convection as the density gradient is stable. Most of the change in the heat transfer occurs in the range $0 < \phi < \pi/2$ where the cavity is heated from the top. Also, it is noticed that the Nusselt number is a strong

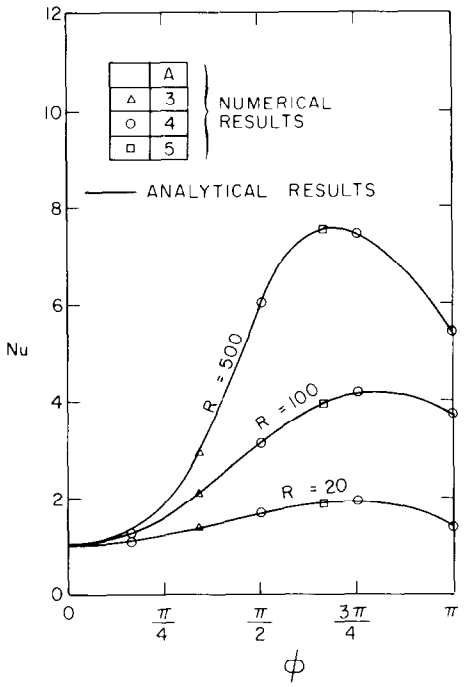

FIG. 2. Effect of inclination angle ϕ on the Nusselt number Nu.

function of the Rayleigh number. As the inclination angle ϕ is increased above $\pi/2$, the enclosure starts to be heated from the bottom. The Nusselt number continues to increase with increasing ϕ, passes through a peak and then begins to decrease. The effect of heating the cavity from the top $0 < \phi < \pi/2$ on the Nusselt number is seen to be large in comparison with that of heating from the bottom $\pi/2 < \phi < \pi$. It is also noticed that the effect of inclination angle on Nusselt number is more pronounced as the Rayleigh number is increased. The peak in Nusselt number occurs at about 125° for $R = 500$ but it is at about 135° for $R = 20$. Therefore, the peak in Nusselt number takes place at a lower inclination angle when Rayleigh number is increased. A similar trend has been reported in the case of inclined fluid cavities containing two opposite isothermal surfaces maintained at different temperatures [20–22].

The maximum value of the streamfunction ψ_{max} and the velocity profiles at a position $x = 0$ as a function of the inclination angle ϕ and Rayleigh number R are presented in Figs. 3 and 4, respectively. The curves illustrate the fact that the convection becomes more and more vigorous as the orientation angle of the cavity is increased. It is observed from Fig. 3 that the curves for ψ_{max} reach a maximum value when the cavity is heated from the bottom. However, contrary to the results obtained for the Nusselt number, the peak in the maximum streamfunction shifts towards $\phi = \pi$ as the Rayleigh number is increased. A similar trend has been reported in the past by Robillard *et al.* [23] while considering the natural convection heat

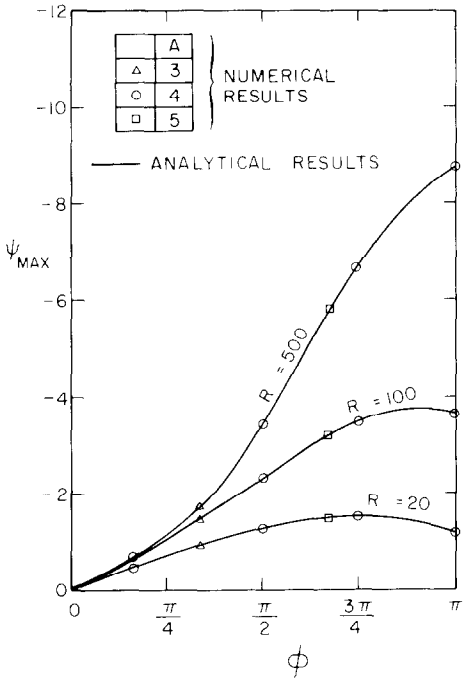

FIG. 3. Effect of inclination angle ϕ on the maximum value of streamfunction ψ_{max}.

transfer within an annular porous layer having its inner boundary isothermal and its outer boundary subjected to a thermal stratification arbitrarily oriented with respect to the gravity. From Fig. 4 it is seen that the velocity is maximum at a position $\phi \approx 3\pi/4$ which corresponds, as discussed previously, with the maximum in the heat transfer rate. In both Figs. 3 and 4 the numerical results are seen to be in excellent agreement with the analytical solution.

As mentioned before, Bories and Combarnous [8] have reported an experimental study of thermal convection in a three-dimensional, tilted, porous box bounded by two parallel, impermeable planes maintained at different temperatures. Several types of flow were observed: a unicellular two-dimensional motion and a juxtaposition of longitudinal coils or polyhedral cells. In particular, three-dimensional hexagonal cells were observed for tilt angles smaller than 15°. Caltagirone and Bories [13] have demonstrated that the above experimentally observed structure can be predicted by a three-dimensional numerical model. For the present case of an inclined layer heated by a constant heat flux, no experimental or three-dimensional results have been reported in the literature. Nevertheless, the rich variety of flow patterns described above can reasonably be also expected to occur. The analytical and numerical results presented here on the basis of a parallel flow are expected to closely predict the appearance of the two-dimensional flow regime but are obviously unable to predict the three-dimensional patterns.

4.1. *The vertical layer heated from the side*

The case of a vertical layer heated from the side with a constant heat flux is of practical interest. For this particular position $\phi = \pi/2$, $\alpha^2 = RC$ and equations (4.6)–(4.8), (4.10) and (4.12) reduce to

$$T = Cx + \frac{\sinh \alpha y}{\alpha \cosh \alpha/2}, \qquad Nu = \frac{\alpha}{2}\coth \alpha/2 \tag{4.14}$$

$$\psi = \frac{R}{\alpha^2}\left[\frac{\cosh \alpha y}{\cosh \alpha/2} - 1\right], \qquad u = \frac{R}{\alpha}\frac{\sinh \alpha y}{\cosh \alpha/2} \tag{4.15}$$

$$C = \frac{R}{2\alpha^3}\left[\frac{\sinh\alpha - \alpha}{\cosh^2 \alpha/2}\right]. \tag{4.16}$$

The boundary layer regime inside a vertical porous

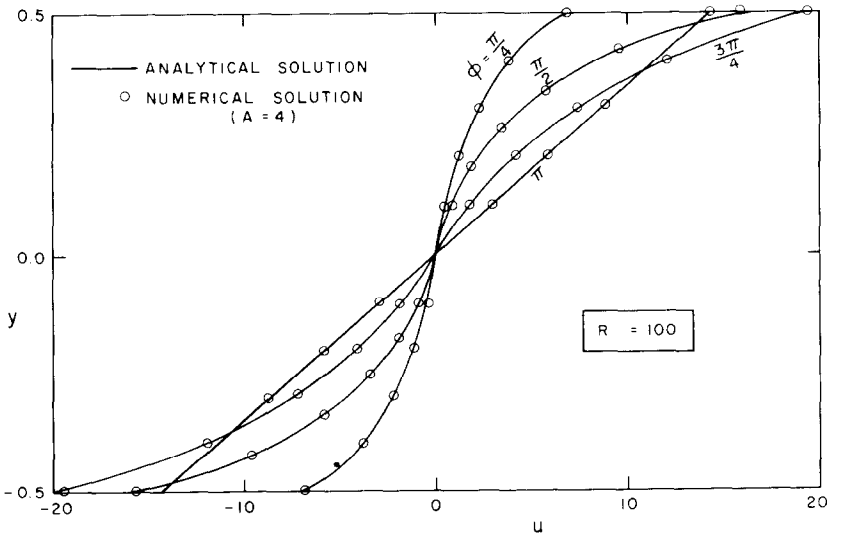

FIG. 4. Effect of inclination angle ϕ on velocity profiles at $x = 0$ for $A = 4$ and $R = 100$.

cavity with uniform heat flux from the side has been studied recently by Bejan [15]. The boundary-layer equations were solved by simplifying the convective transport terms in the energy equation in a way analogous to that accomplished by the method of Oseen linearization in the analysis of low Reynolds number flows. The resulting velocity and temperature fields in the vicinity of the vertical walls was found to be exponentially varying. It was also demonstrated that the vertical boundary-layer thickness is constant with altitude and the core region inside the cavity is motionless and linearly stratified. It is interesting to note that Bejan's solution may be recovered as a limit case of the present study. Hence when $R \gg 1$, it may be easily shown that $\alpha \sim R^{2/5}$, $C \sim R^{-1/5}$ and equations (4.6)–(4.9) and (4.13) reduce to:

$$T = \frac{x}{\sqrt{\alpha}} + \frac{1}{\alpha} e^{-\alpha \bar{y}} \tag{4.17}$$

$$\psi = \sqrt{\alpha} e^{-\alpha \bar{y}}; \qquad u = \alpha^{3/2} e^{-\alpha \bar{y}} \tag{4.18}$$

$$Nu = \frac{\alpha}{2} \tag{4.19}$$

where $\bar{y} = y - 1/2$.

The above equations are the same as those obtained by Bejan [15] when translated into corresponding notations. It is worthwhile to mention that the equations presented by Bejan in his paper are written explicitly in terms of the aspect ratio A of the cavity. However, as demonstrated by equations (4.17)–(4.19), the aspect ratio is not a parameter in this type of problem and in fact may be eliminated from Bejan's results by a simple renormalization of his equations.

Figure 5 shows the effect of Rayleigh number R on Nusselt number Nu for inclination angle $\phi = \pi/2$ and aspect ratio $2 \leqslant A \leqslant 10$. The present analytical solution, equation (4.14), is compared with the numerical results of Bejan [15] and those obtained in this study. Figure 5 also shows the Nusselt number predicted for the boundary-layer flow regime, equation (4.19). In the case of a slow motion, $R \ll 1$, it may be shown from equations (4.14) and (4.16) that the Nusselt number predicted by the present theory is given by $Nu \approx 1 + R^2/144$. It is seen from Fig. 5 that all results are in good agreement. It is also noticed that the boundary-layer solution, equation (4.19), predicts accurately the Nusselt number for Rayleigh numbers higher than approximately $R = 25$. Finally it must be mentioned that, contradictory to the case of a porous cavity whose vertical walls are isothermally maintained [24], the numerical results obtained in the present study, for a cavity heated by constant heat fluxes, show no dependence on the aspect ratio when $A \geqslant 2$. This point is illustrated in Fig. 5 where the numerical results, obtained for $A = 3$, 4, 5 and 10, are seen to be in good agreement with the aspect ratio independent correlation predicted by equation (4.19). However, as discussed by Bejan [15] and Prasad and Kulacki [24] the structure of the flow and temperature patterns resulting from these two types of boundary conditions are considerably different.

4.2. *The horizontal layer heated from the bottom*

It is of interest to examine the case of a horizontal layer heated from the bottom with a constant heat flux. For this situation $\phi = \pi$ and $\alpha \to 0$, and it may be shown that the flow and temperature fields are given by:

$$T = Cx + y\left[1 + \frac{RC^2}{2}\left(\frac{y^2}{3} - \frac{1}{4}\right)\right] \tag{4.20}$$

$$\psi = \frac{RC}{2}\left(y^2 - \frac{1}{4}\right); \qquad u = RCy \tag{4.21}$$

$$C = \pm \frac{1}{R}\sqrt{10(R - 12)}, \qquad \text{or } C = 0 \tag{4.22}$$

$$Nu = 1/(1/6 + 10/R), \qquad \text{or } Nu = 1. \tag{4.23}$$

From equation (4.22) it is seen that for $Ra \leqslant 12$ the present analysis predicts that no motion may be induced inside the cavity. It is interesting to mention that the onset of convection, induced by buoyancy effects resulting from vertical thermal gradients, in a horizontal layer of a saturated porous medium, has been studied in the past by Nield [25]. Using a linear perturbation analysis the critical Rayleigh numbers for the onset of convection were obtained for various thermal boundary conditions imposed on the boundaries of the horizontal layer. For the case of the boundary conditions considered in the present study, i.e. rigid horizontal walls heated from the bottom and cooled from the top by a constant heat flux, a critical Rayleigh number of $R = 12$ was predicted for the onset of convection. This result is in agreement with the prediction of equation (4.22). Numerical tests, performed for a cavity with aspect ratio $A = 4$, have also shown that for $R < 12$ no convective motion may be induced inside the cavity. For values of $R > 12$ the flow inside the cavity was found to depend upon the Rayleigh number and the initial conditions used to initiate the flow. For instance the numerical results presented in Fig. 6(a) for the case $R = 50$, $A = 4$ and $\phi = 180°$ were obtained by using as initial conditions the steady-state solution indicating a unicellular flow regime obtained previously with the same parameters but at an inclination angle $\phi = 175°$. A steady-state unicellular flow was obtained and the resulting velocity profile depicted in Fig. 4 is seen to be in excellent agreement with that predicted by the present theory. However, this type of flow does not seem to have been observed experimentally in the past. On the other hand when pure conduction temperature profiles with no motion were used as initial conditions it was found that a steady-state multicellular flow pattern (Fig. 6(b)) was induced by the roundoff errors generated in the numerical computations. Also it

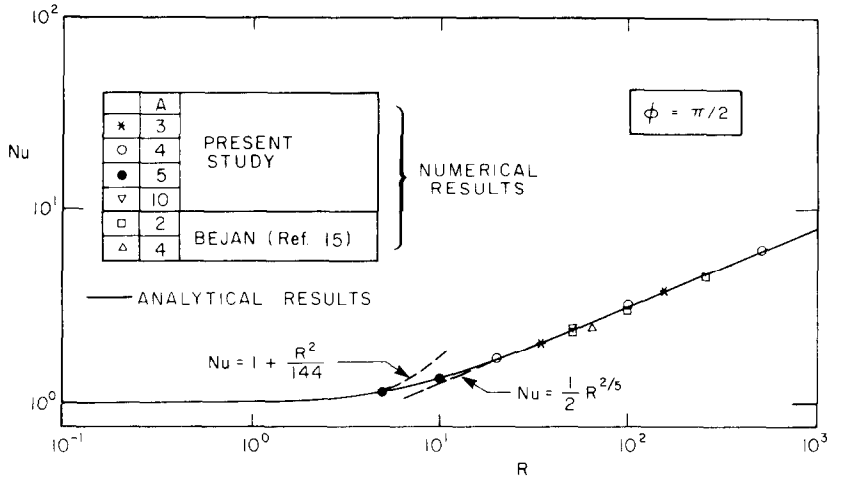

FIG. 5. Effect of Rayleigh number R on the Nusselt number Nu for a vertical cavity ($\phi = \pi/2$) heated from the side.

should be mentioned that, for very high values of the Rayleigh number, no steady unicellular flow could be maintained inside the cavity independently of the initial conditions used to start the flow. In fact, when the angle of inclination is approaching 180°, the flow might not be two-dimensional as assumed in the theoretical and numerical solutions. For instance, experimental observations and three-dimensional numerical simulations have shown that, in the case of a tilted, porous, rectangular cavity, the flow remains two-dimensional for $0 < \phi < 173°$ but for $\phi \geqslant 173°$, oblique rolls were obtained [8]. The multicellular flow pattern depicted in Fig. 6b is similar to the classical Bénard cells observed in a confined porous medium heated from below at a constant temperature. For this situation it was found by Lapwood that the critical Rayleigh number at which the heat transport process changes from purely conductive to convective transfer was $R = 4\pi^2$, i.e. approximately three times higher than the value $R = 12$ reported by Nield [25] for the present situation. It is also observed in Fig. 6(b) that, due to the thermal boundary conditions considered in this study, the temperature on the horizontal planes is not uniform but rather varies periodically from a maximum to a minimum value.

Figure 7 shows a comparison between the theoretical Nusselt number predicted by equation (4.23) and numerical results obtained for cavities with aspect ratios $A = 2$, 3 and 4. In all the numerical results presented in Fig. 7 the flow inside the cavity was steady and unicellular.

5. LAYER HEATED FROM THE END WALLS

In this section we consider the case where a constant heat flux is imposed on the end walls of the porous layer while its side walls are maintained adiabatic. To this end, the constant heat flux imposed on the side walls in Fig. 1 is replaced by adiabatic conditions and the end walls are now subjected to a constant heat flux. For this situation the flow and temperature fields are described by equations (2.9) and (2.10) subjected to the following boundary conditions:

$$\psi = 0 \qquad \frac{\partial T}{\partial x} = 1 \qquad \text{on } x = \pm A/2 \tag{5.1}$$

$$\psi = 0 \qquad \frac{\partial T}{\partial y} = 0 \qquad \text{on } y = \pm 1/2. \tag{5.2}$$

Proceeding as in Section 4 it may be shown that the solution for the temperature field, streamfunction and velocity profiles are given by equations (4.6), (4.7) and (4.9) respectively where the constant B is now given, for the present situation, by

$$B = -C\cot\phi/\cosh\alpha/2. \tag{5.3}$$

Integrating the energy equation (2.10) over the control volume of Fig. 1 and making use of the boundary conditions (5.1) and (5.2) one obtains:

$$\int_{-1/2}^{1/2} \left(uT - \frac{\partial T}{\partial x}\right) dy = -1. \tag{5.4}$$

Substituting equations (4.6), (4.9), (5.3) into (5.4) and integrating yields:

$$C = 1 - \frac{B\cot\phi}{\alpha}\left[\frac{(\sinh\alpha - \alpha)}{2\cosh\alpha/2} + (2\sinh\alpha/2 - \alpha\cosh\alpha/2)\right]. \tag{5.5}$$

Figure 8 presents the maximum value of the streamfunction ψ_{max} as a function of the inclination angle ϕ for Rayleigh numbers R of 20, 50 and 100 as predicted by equations (4.7), (5.3) and (5.5). Also shown in Fig. 8 are results of numerical calculations for cavities with aspect ratios $A = 3$, 4 and 5. The effect of inclination angle ϕ on temperature profiles at $x = 0$ for $A = 4$ and $R = 100$ is illustrated in Fig. 9. A good agreement between the analytical and numerical

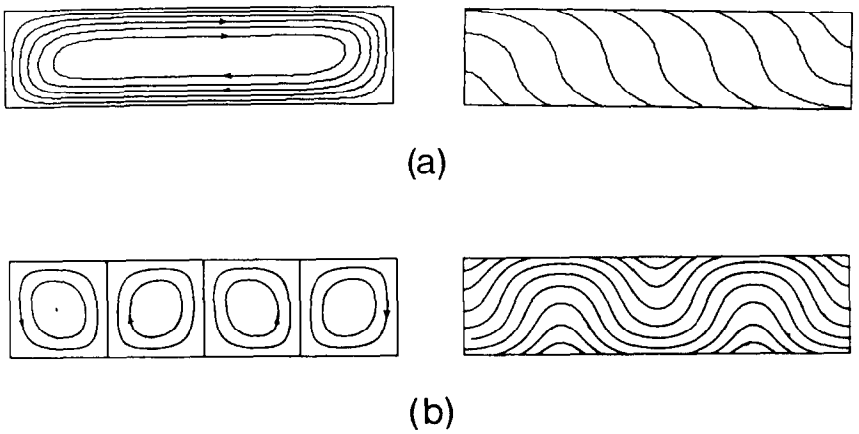

FIG. 6. Streamlines and isotherms for a horizontal layer heated from the bottom ($\phi = \pi$) for $A = 4$ and $R = 50$.

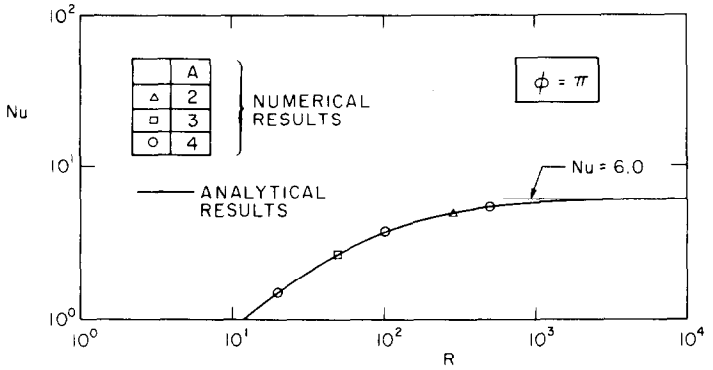

FIG. 7. Effect of Rayleigh number R on the Nusselt number Nu for a horizontal cavity ($\phi = \pi$) heated from the bottom.

results is observed. It must be mentioned at this stage that the Nusselt number Nu predicted by the present theory, for the case of a layer heated from the end walls, was not found to be in good agreement with the results of the numerical solution, especially when the Rayleigh numbers are large. This is due to the fact that the Nusselt number, defined by equation (4.13), is based on the knowledge of the averaged temperature difference between the two heated walls. However the theoretical temperature distribution given by equations (4.6), (5.3) and (5.5) is valid only in the core region of the cavity and becomes a very poor approximation in the end regions near the heated walls. Hence a good agreement between the theoretical and the numerical Nusselt numbers cannot be expected.

For the case of a horizontal layer heated from the side $\phi = 0$ and $\alpha \to 0_1$ it may be shown from equations (4.6), (4.7), (4.9), (5.3) and (5.5) that the temperature and flow fields are described by

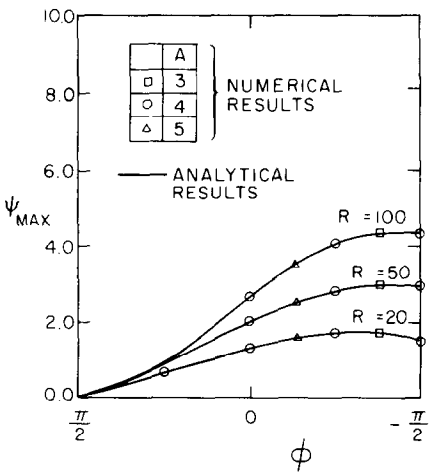

FIG. 8. Effect of inclination angle ϕ on the maximum value of streamfunction ψ_{max}.

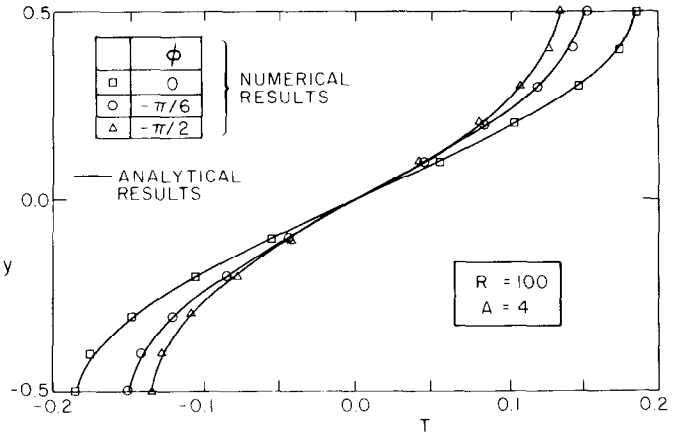

FIG. 9. Effect of inclination angle ϕ on temperature profiles at $x = 0$ and $A = 4$ and $R = 100$.

$$T = Cx - \frac{RC^2}{2} y\left(\frac{y^2}{3} - \frac{1}{4}\right) \tag{5.6}$$

$$\psi = -\frac{RC}{2}\left(y^2 - \frac{1}{4}\right); u = -RCy \tag{5.7}$$

where the value of C is given by

$$C^3R^2 + 120C - 120 = 0. \tag{5.8}$$

This problem has been studied recently by Vasseur *et al.* [19] for a wide range of Rayleigh numbers $10^{-1} \leqslant R \leqslant 10^3$ and aspect ratios $10 \leqslant A \leqslant 3$. It was demonstrated that the above analytical solution was in good agreement with a numerical solution of the full governing equations (2.9)–(2.13) provided that both the Rayleigh number and the inverse of the aspect ratio be relatively not too large. For instance, when $A = 4$, the flow was demonstrated to remain parallel for $R \leqslant 625$. As the aspect ratio of the cavity is increased, the maximum Rayleigh number for which the flow maintains its parallel character also increases. Also, the existence of multicellular flows similar to those observed numerically by Prasad and Kulacki [24] and experimentally by Ostrach *et al.* [27] in their study of natural convection in shallow cavities bounded by isothermal vertical walls, has been discussed in ref. [19]. It was found in particular that, relative to the case where the temperature is specified along the side walls, the imposition of temperature derivative (q') has a stabilizing effect on the flow structure. As a result, with the present boundary conditions, the flow structure becomes multicellular for Rayleigh numbers approximately three orders of magnitude higher than the values reported by ref. [24] for shallow cavities isothermally heated from the side.

It is also of interest to consider the case of a vertical, porous layer heated from the bottom with a constant heat flux. For this situation $\phi = -\pi/2$ and $\alpha^2 = RC$, and it may be shown that:

$$T = \frac{\pi^2}{R} x + D \sin \pi y \tag{5.9}$$

$$\psi = \frac{DR}{\pi} \cos \pi y; \qquad u = -DR \sin \pi y \tag{5.10}$$

where the value of D is given by

$$D = \pm\sqrt{2(R - \pi^2)}/R, \qquad \text{or } D = 0. \tag{5.11}$$

From equation (5.11) it is predicted that a convective motion inside the cavity may be generated only for $R > \pi^2$. This critical Rayleigh number for the onset of convection has been verified numerically and it was found that, for $R < \pi^2$, the fluid was indeed motionless and thermally stratified. However, as illustrated in Fig. 10, for $R > \pi^2$, a flow field is induced inside the cavity resulting in a single cell circulating clockwise or counterclockwise depending on the roundoff errors generated in the numerical computations.

Figure 11 presents a comparison between the theoretical sinusoidal velocity profiles predicted by equation (5.10) at the position $x = 0$ and the numerical results for $R = 20$, 50 and 100 and $A = 4$. A good agreement between both results is observed.

6. CONCLUSIONS

The problem of natural convection in a two-dimensional, inclined porous layer with uniform heat flux from two opposite walls while the other walls are insulated has been studied both numerically and theoretically. An approximate analytical solution was obtained by assuming the natural convection pattern to consist of a core region situated in the middle of the porous layer in addition to the two end regions. When the aspect ratio of the cavity is large ($A \gg 1$) the streamlines in the core region are essentially parallel to the boundaries of the cavity. The main conclusions of the present analysis are:

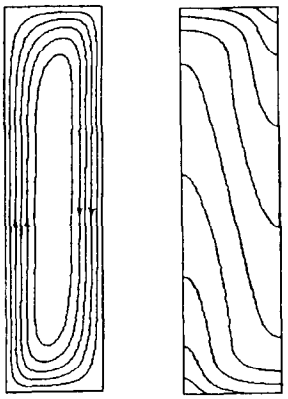

FIG. 10. Streamlines and isotherms for a vertical layer heated from the bottom ($\phi = -\pi/2$) for $A = 4$ and $R = 100$.

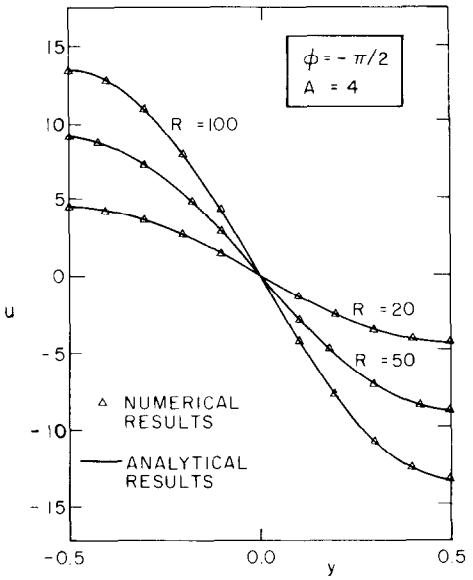

FIG. 11. Effect of Rayleigh number R on velocity profiles at $x = 0$ for a vertical layer heated from the bottom ($\phi = -\pi/2$).

6.1. *Cavity heated from the long side walls*

(i) The orientation of the cavity has, for a given Rayleigh number, a large effect on the heat transfer rate. The maximum heat transfer occurs when the enclosure is heated from the bottom $90° < \phi < 180°$. As the Rayleigh number increases the angle at which maximum energy transfer takes place shifts towards lower values of ϕ.

(ii) In the case of a vertical layer heated from the side ($\phi = 90°$) the temperature and velocity fields predicted by the present study for boundary-layer regime ($R \gg 1$) are in agreement with Bejan's solution [15] obtained by solving the boundary-layer equations by a linearization technique.

(iii) In the case of a horizontal layer heated from the bottom ($\phi = \pi$) the present theory indicates that no flow can be initiated when $R \leqslant 12$. A similar result has been predicted in the past by Nield [25] on the basis of a stability analysis. For $R > 12$ both unicellular and multicellular flows may be observed in the cavity, depending on the Rayleigh number, aspect ratio and initial conditions used to initiate the flow.

6.2. *Cavity heated from the short end walls*

(i) The effect of the orientation angle on the flow field was found to be similar to that observed for the cavity heated from the long side walls.

(ii) In the case of a vertical layer heated from the bottom ($\phi = -\pi/2$) the present theory predicts a motionless fluid when $R < \pi^2$. This critical Rayleigh number for the onset of convection has been confirmed by numerical simulations.

The main features of the approximate theoretical solution have been tested by a numerical solution of the full governing equations in the range $20 \leqslant R \leqslant 50$, $2 \leqslant A \leqslant 10$ and $0 \leqslant \phi \leqslant \pi$ for the cavity heated from the long side walls and $-\pi/2 \leqslant \phi \leqslant \pi/2$ for the cavity heated from the short end walls. Finally, it should be noted that the scope of this study is limited by the assumption of two-dimensional steady laminar flow, i.e. nothing can be inferred about the possible development of various types of instabilities that could lead to an unsteady and/or three-dimensional flow within the range of Rayleigh numbers and inclination angles considered in the present study.

Acknowledgements—This work was supported in part by the Natural Sciences and Engineering Research Council of Canada through grants A-9201 and A-4197 and jointly by the FCAC Government of Quebec, under grant CRP 507-78. The authors gratefully thank Ecole Polytechnique for providing the necessary time on an IBM 4381 computer.

REFERENCES

1. M. A. Combarnous and S. A. Bories, Hydrothermal convection in saturated porous media. In *Advances in Hydroscience*, Vol. 10, pp. 231–307 (1975).
2. I. Catton, Natural convection in enclosures, *Proc. 6th Int. Heat Transfer Conference*, Toronto, Vol. 6, pp. 209–235 (1979).
3. P. J. Burns, L. C. Chow and C. L. Tien, Convection in a vertical slot filled with porous insulation, *Int. J. Heat Mass Transfer* **20**, 919–926 (1976).
4. J. Weber, The boundary layer regime for convection in a vertical porous layer, *Int. J. Heat Mass Transfer* **18**, 569–573 (1979).
5. G. S. Shiralkar, M. Haajizadeh and C. L. Tien, Numerical study of high Rayleigh number in a vertical porous enclosure, *Numer. Heat Transfer* **6**, 223–234 (1983).
6. J. W. Elder, Convection in a porous medium with horizontal and vertical temperature gradients, *Int. J. Heat Mass Transfer* **17**, 241–248 (1974).
7. N. Rudraiah and T. Masuoka, Asymptotic analysis of natural convection through horizontal porous layer, *Int. J. Engng Sci.* **20**, 27–39 (1982).
8. S. A. Bories and M. A. Combarnous, Natural convection in a sloping porous layer, *J. Fluid Mech.* **57**, 63–79 (1973).
9. M. P. Vlasuk, Convection heat transfer in a porous layer, *4th All-Union Heat Mass Transfer Conference*, Minsk (1972).
10. P. H. Holst and K. Aziz, Transient natural convection in confined porous media, *Int. J. Heat Mass Transfer* **15**, 73–90 (1972).

11. J. P. Walch and B. Dulieu, Convection naturelle dans une boîte rectangulaire légèrement inclinée contenant un milieu poreux, *Int. J. Heat Mass Transfer* **22,** 1607–1612 (1979).
12. S. L. Moya, E. Ramos and M. Sen, Numerical study of natural convection in a tilted rectangular porous material, *Int. Heat Mass Transfer* (1987), in press.
13. J. P. Caltagirone and S. Bories, Solutions and stability criteria of naturel convective flow in an inclined porous layer, *J. Fluid Mech.* **155,** 267–287 (1985).
14. V. Prasad and F. A. Kulacki, Natural convection in a rectangular porous cavity with constant heat flux on one vertical wall, *J. Heat Transfer* **106,** 152–157 (1984).
15. A. Bejan, The boundary layer regime in a porous layer with uniform heat flux from the side, *Int. J. Heat Mass Transfer* **26,** 1339–1346 (1983).
16. D. W. Peaceman and H. A. Rachford, The numerical solution of parabolic and elliptic difference equations, *J. Soc. Ind. appl. Math.* **3,** 28–43 (1955).
17. K. L. Walker and G. M. Homsy, Convection in a porous cavity, *J. Fluid Mech.* **87,** 449–474 (1978).
18. A. Bejan and C. L. Tien, Natural convection in a horizontal porous medium subjected to an end-to-end temperature difference, *J. Heat Transfer* **100,** 191–198 (1978).
19. P. Vasseur, L. Rubillard and I. Anochiravani, Natural convection in a shallow porous cavity heated from the side with a uniform heat flux, *Chem. Engng Commun.* **46,** 129–146 (1986).
20. H. Ozoe, H. Sayama and S. W. Churchill, Natural convection in a long inclined rectangular box heated from below, *Int. J. Heat Mass Transfer* **20,** 123–129 (1977).
21. C. J. Chen and V. Talaie, Finite analytic numerical solutions of laminar natural convection in two-dimensional inclined rectangular enclosures, *National Heat Transfer Conference*, Denver, CO, paper 85-HT-10 (1985).
22. H. Inaba and K. Kanayama, Natural convective heat transfer in an inclined rectangular cavity, *Bull. J.S.M.E.* **27,** 1702–1708 (1984).
23. L. Robillard, T. H. Nguyen and P. Vasseur, Free convection in a two dimensional porous loop, *J. Heat Transfer* **108,** 277–283 (1986).
24. V. Prasad and F. A. Kulacki, Convective heat transfer in a rectangular porous cavity—effect of aspect ratio on flow structure and heat transfer, *J. Heat Transfer* **106,** 158–165 (1984).
25. D. A. Nield, Onset of thermohaline convection in a porous medium, *Water Resour. Res.* **4,** 535–560 (1968).
26. E. R. Lapwood, Convection of a fluid in a porous medium, *Proc. Camb. Phil. Soc.* **44,** 508–521 (1948).
27. S. Ostrach, R. R. Loka and A. Kumar, Natural convection in low aspect-ratio rectangular enclosures, *19th National Heat Transfer Conference*, Orlando, FL. *Natural Convection in Enclosures*, HTD-Vol. 8, pp. 1–10. ASME, New York (1980).

CONVECTION NATURELLE DANS UNE COUCHE POREUSE, MINCE, INCLINEE, EXPOSEE A UN FLUX DE CHALEUR CONSTANT

Résumé—On étudie analytiquement et numériquement une cavité rectangulaire mince, inclinée, remplie par un milieu poreux saturée de fluide. Un flux thermique constant est appliqué pour chauffer et refroidir les deux parois opposées de la couche, tandis que les autres parois sont isolées. Sur la base des équations de Darcy–Oberbeck–Boussinesq, le problème est résolu analytiquement, dans la couche mince, en utilisant un développement asymptotique, et une forme intégrale de l'équation d'énergie. Des solutions pour les deux champs, distributions de température et nombres de Nusselt sont obtenus explicitement en fonction du nombre de Rayleigh et de l'angle d'inclinaison de la cavité. Une étude numérique du même phénomène est conduite en résolvant le système complet des équations de base. Un bon accord est trouvé entre les calculs analytiques et la simulation numérique.

NATÜRLICHE KONVEKTION IN EINER DÜNNEN, GENEIGTEN, PORÖSEN SCHICHT BEI KONSTANTER WÄRMESTROMDICHTE

Zusammenfassung—Die natürliche Konvektion in einem dünnen, rechteckigen und geneigten Hohlraum, der mit einer überfluteten Schüttung gefüllt ist, wird analytisch und numerisch untersucht. Die beiden gegenüberliegenden Wände werden mit konstanter Wärmestromdichte geheizt bzw. gekühlt, während die beiden anderen Wände wärmegedämmt sind. Auf der Grundlage der Darcy–Oberbeck–Boussinesq Gleichungen wird das Problem für eine dünne Schicht analytisch mit Hilfe der asymptotischen Näherung und einer Integralform der Energiegleichung gelöst. Lösungen für die Stromlinienfelder, Temperaturverteilungen und Nusselt-Zahlen werden explizit als Funktion der Rayleigh-Zahl und des Neigungswinkels ermittelt. Eine numerische Untersuchung desselben Phänomens, der eine vollständige Lösung der beschreibenden Gleichungen zugrundeliegt, wurde ebenfalls durchgeführt. Gute Übereinstimmung zwischen analytischen und numerischen Ergebnissen wurde erreicht.

ЕСТЕСТВЕННАЯ КОНВЕКЦИЯ В ТОНКОМ НАКЛОННОМ ПОРИСТОМ СЛОЕ ПРИ ПОСТОЯННОМ ТЕПЛОВОМ ПОТОКЕ

Аннотация—Аналитически и численно исследуется вызванное разностью температур течение в наклонной прямоугольной полости небольшой высоты, заполненной насыщенным жидкостью пористым материалом. Одна из двух противоположных стенок полости нагревается, а вторая—охлаждается постоянным тепловым потоком, в то время как две другие стенки теплоизолированы. Из уравнений Дарси–Обербека–Буссинеска получено аналитическое решение задачи в приближении тонкого слоя с использованием асимптотических разложений и интегральной формы уравнения энергии. Решения для полей течения, распределений температур и различных значений числа Нуссельта даны в явном виде в зависимости от числа Рэлея и угла наклона полости. Проведено также исследование этой же задачи на основе численного решения полной системы основных уравнений. Получено хорошее соответствие между результатами аналитических расчетов и численного моделирования.